Botanica SERBICA 39 (2): (2015) 137-142

Original Scientific Paper

Estimation of meristemoid complexity during *Tacitus bellus in vitro* shoot organogenesis by 2D fractal analysis

Sladjana Z. Spasić[1]*, Aleksandra Lj. Mitrović[1], Dušica Janošević[2] and Snežana Budimir[3]

1 Institute for Multidisciplinary Research, Department of Life Sciences, University of Belgrade, Kneza Višeslava 1, 11030 Belgrade, Serbia

2 Institute of Botany and Botanical Garden "Jevremovac", Faculty of Biology, University of Belgrade, Takovska 43, 11000 Belgrade, Serbia

3 Institute for Biological Research "Siniša Stanković", University of Belgrade, Bulevar despota Stefana 142, 11060 Belgrade, Serbia

ABSTRACT: This study considered the analysis of 2D fractal characteristics of cell populations that participate in meristemoid formation during the process of *de novo* shoot organogenesis in *Tacitus bellus* leaf explant culture. Micrographs representing early and late meristemoid formation stages were used for 2D fractal analysis. Analysis showed that meristemoid complexity at two selected points of development were characterized by significantly different fractal dimension values. This result demonstrates that the proposed method is efficient for the fine distinction of histologically similar structures at an appropriate resolution of micrographs.

Keywords: 2D Fractal Dimension; Shoot Organogenesis; *Tacitus bellus*

Received: 15 March 2015 Revision accepted 29 May 2015

UDK 581.8

INTRODUCTION

Fractals are described as self-similar or self-affine patterns, from exactly the same at every scale, to nearly the same at different scales. Their complexity is due to infinite repeating details within details. Mandelbrot (1975) proposed the term "fractal dimension" (*FD*) to qualify objects with the same structure at all scales. Mathematical objects are self-similar over an unlimited range of scales, whereas biological components are statistically self-similar only within a fractal domain defined by limits (Losa 2011). Self-similar objects are common in Nature and thus their precise characterization is of great importance (Mandelbrot 1982). Jelinek & Fernandez (1998) showed that in different fields of science and especially in botany, where variability is the rule rather than a coincidence, it is necessary to apply different fractal methods to obtain a complete picture of structures or processes. Hausdorff's dimension, also known as the similarity dimension, has been successfully applied for the identification of leaf complexity (Bruno et al. 2008), while the Minkowski fractal dimension was used for leaf shape analysis (de Oliveira Plotze *et al.* 2005). The box-counting dimension enabled discrimination between individuals of *Anthyllis cytisoides* by comparing branch architecture (Alados *et al.* 1999) and to characterize xylem differentiation in *Populus* X*euramericana* plants (Xi & Zhao 2011).

Expansion of the concepts of fractal geometry towards the life sciences has led to significant progress in analytical morphology, microscopy and histopathology, in understanding the complex architectural, morphological or structural features that characterize cells and tissues during ontogenesis or in developmental processes, both normal and pathological (Landini 2011). Fractal analysis has found applications in properties of tumors, blood

*correspondence: sladjana@imsi.rs, sladjana@ibiss.bg.ac.rs

vessels and neurons, viral infections, and detection of coding DNA regions (Cross 1997).

In plants, *de novo* shoot and root organogenesis relies on tipotency of special populations of cells that can be considered adult stem cells (Sugimoto *et al.* 2011). During direct shoot organogenesis, shoot meristems arise from stem cells in different explant types (hypocotyls, stem and leaf) as the result of repeated cell divisions. The cells within the meristem could be regarded as self-similar objects, fractals.

In *Tacitus bellus* leaf explant culture, shoot organogenesis involves three distinct morphogenic stages: initiation of shoot organogenesis, meristemoid formation and shoot bud formation (Mitrović et al. 2012). A new numerical method for 2D fractal dimension estimation provided numerical quantification of these morphogenetic stages (Spasić 2014). In the current work, we examined the precision of 2D fractal dimension estimation in quantification of cell organization complexity within the meristemoid formation stage of *T. bellus* shoot organogenesis. Additionally, we determined the preferable resolution for use in 2D fractal dimension analysis in quantifications of plant histological structures complexity.

MATERIAL AND METHODS

Plant material: *Tacitus bellus* (L.) Moran and J. Meyrán, syn. *Graptopetalum bellum* lower rosette leaves excised from plants *in vitro* were used as explants for the induction of direct shoot organogenesis. Leaf explants were further cultured on MS (Murashige & Skoog 1962) medium supplemented with benzyladenine (BAP) at 0.1 mg dm^{-3} and α-naphthaleneacetic acid (NAA) at 0.1 mg dm^{-3} according to procedures reported by Mitrović *et al.* (2005) and Mitrović *et al.* (2012). Cultures were maintained with a photoperiod of 16 h light under an irradiance of 70 μmol m^{-2} s^{-1}, at 25 ± 2 °C. Four replicates of 5 explants collected at the 20th and 30th days from culture initiation were used for histological examination.

Microscopy: Explants were fixed in formalin + acetic acid + ethanol (10:5:85) solution, dehydrated in a graded ethanol series and embedded in paraffin wax at 58 °C. Sections (8 μm thick) were stained with haematoxylin and photographed under a Leitz DMRB photomicroscope (Leica, Wetzlar, Germany, 10x objective).

Micrograph preparation for fractal analysis: For the fractal analysis we selected 6 micrographs representing early (20th day after culture initiation) (Fig. 1A) and late (30th day after culture initiation) (Fig. 1F) meristemoid stages. The original micrographs (each at 3 resolutions: 96, 192, and 384 pixel/inch) were converted to gray scale and auto contrast correction was performed using Adobe Photoshop 7.0. The "informative part", representing the specific stage of shoot bud formation with an adequately small part of surrounding tissue of primary leaf explant, was cropped (Fig. 1 B, G). The size of these new images, prepared for the analysis, was 14 x 8 inches (for example, at a resolution of 96 pixel/inch: 1344 x 768 pixels or 1032192 points).

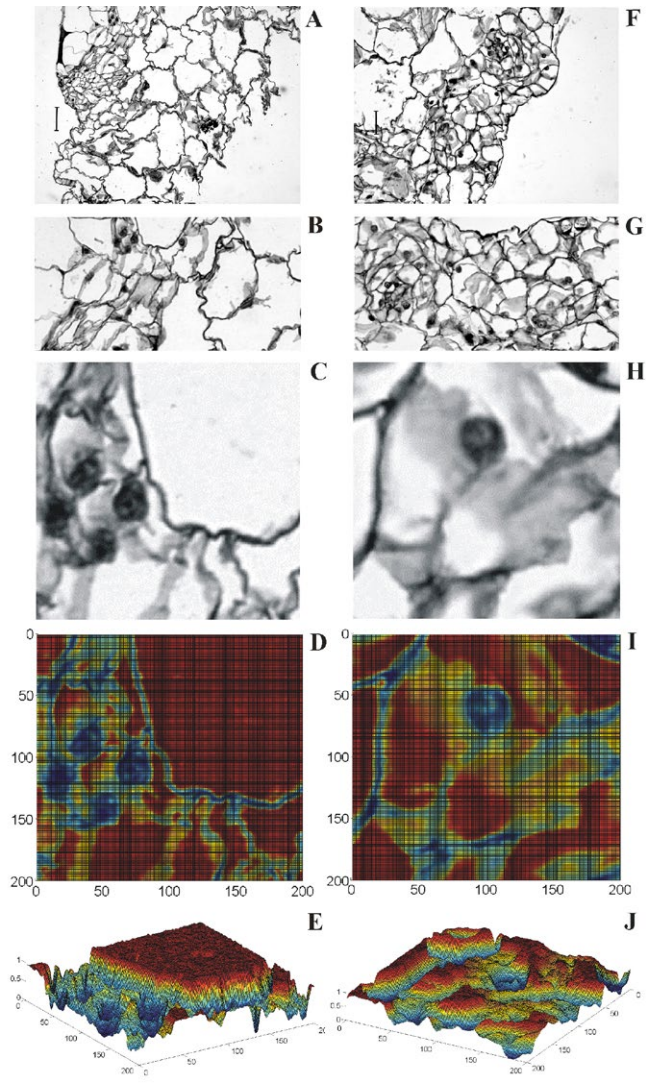

Figure 1. *T. bellus* direct shoot organogenesis from leaf explants: meristemoids (A–E) - at the 20th day and (F–J) – at the 30th day from culture initiation; A) and F) – the original micrographs of cross sections of explants, converted to gray scale, (*bar* = 80 μm); B) and G) - the "informative part" of the micrograph (14 x 8 inches), representing the specific stage of shoot bud formation with surrounding tissue of primary leaf explant; C) and H) - four square windows (each 100x100 points dimension) of sample images excised from B) and G), respectively; D) and I) - numerical matrix representation corresponding to C) and H) respectively; E) and J) - surface representation of D) and I) respectively. *FD* values of histological images are calculated using their corresponding numerical matrix by application our new method with parameters N=100, M=100 and k_{max} = 8.

In the first step of image processing, gray scale images were converted into the matrices with elements in real interval [0, 1]. The intensity image was converted to a numeric field, rescaling the data to numeric value in R[0,] so that: black was converted to 0 and white to 1. Finally, for each image, the resulting matrix with elements in R[0,1] was obtained. Thereafter the resulting matrices were subjected to calculating *FD*.

A method for calculating 2D fractal dimension: Fractal analysis of histological images was performed by the new numerical method for calculating the 2D fractal dimension (*FD*) of a surface described in detail by Spasić (2014).

Let $\mathbf{X}$ be a (M x N)-dimensional matrix where $\boldsymbol{x}_{ij}$ are its elements and i=1,…, M, j=1,…, N. Then, the matrix X can be seen as a discrete representation of the function f, a surface in 3-dimensional Euclidean space. A graph of the function f, $G(f)$ is the set of points $(i, j, \boldsymbol{x}_{ij})$ in R^3, i=1,…, M, j=1,…, N, where $\boldsymbol{x}_{ij} = f(i,j)$.

We linked into triangles, three by three, the points of the graph $G(f)$ corresponding to the coordinates (i, j) on the xy grid. We chose the step equal to one, meaning that we took all the points $(i, j, \boldsymbol{x}_{ij})$ into account. The set of triangles formed in that way approximated the surface f. We could therefore approximate the area of the surface f by the sum of the areas of the resulting triangles. We then increased the step size and repeated the process. For the step size equal to two we chose every second point from the starting matrix $\mathbf{X}$ along rows and columns forming a new matrix, etc.

Formally, let $k_{max,}$ be a free parameter representing the maximum step size. For k=1,…,k_{max}, let us construct k new matrices $\mathbf{X}_k^m$ as:

$$\mathbf{X}_k^m = \begin{bmatrix} x_{m,m} & x_{m+k,m} & x_{m+2k,m} & \cdots & x_{m+pk,m} \\ x_{m,m+k} & x_{m+k,m+k} & x_{m+2k,m+k} & \cdots & x_{m+pk,m+k} \\ \cdots & \cdots & \cdots & \cdots & \cdots \\ x_{m,m+sk} & x_{m+k,m+sk} & x_{m+2k,m+sk} & \cdots & x_{m+pk,m+sk} \end{bmatrix} \tag{1}$$

where m=1, 2,…, k, $p = \text{int}[(M-m)/k]$, $s = \text{int}[(N-m)/k]$, and int(r) is the integer part of the real number r. In that way, for k=2 we formed the new matrix $\mathbf{X}_2^m$, for k=3 we formed matrix $\mathbf{X}_3^m$,... and so on up to the k=k_{max}.

Then, we approximated the surface f by triangles whose vertexes were given by the matrices $\mathbf{X}_k^m$. The sum of the areas of triangles, $A_m(k)$, was computed for each of the k matrix $\mathbf{X}_k^m$ representing surfaces:

$$A_m(k) = C\sum_{i=1}^{\left[\frac{M-m}{k}\right]}\sum_{j=1}^{\left[\frac{N-m}{k}\right]}\left\{\left|x_{m+(i-1)k,m+jk} - x_{m+(i-1)k,m+(j-1)k}\right|\cdot\left|x_{m+ik,m+jk} - x_{m+(i-1)k,m+jk}\right| + \left|x_{m+ik,m+jk} - x_{m+ik,m+(j-1)k}\right|\cdot\left|x_{m+ik,m+(j-1)k} - x_{m+(i-1)k,m+(j-1)k}\right|\right\} \tag{2}$$

where $C = \dfrac{1}{2k^4}\dfrac{(N-1)}{\left[\frac{N-m}{k}\right]}\dfrac{(M-1)}{\left[\frac{M-m}{k}\right]}$.

$A_m(k)$ was averaged for all m, forming the mean value of the surface area $A(k)$ for each k=1,...,k_{max} as

$$A(k) = \frac{\sum_{m=1}^{k} A_m(k)}{k} \tag{3}$$

An array of mean values $A(k)$ was obtained, with S the slope of the least squares linear best fit from the plot of $\ln(A(k))$ versus $\ln(1/k^2)$:

$$S = \ln(A(k))/\ln(1/k^2). \tag{4}$$

The *FD* was estimated as

$$FD = S+1. \tag{5}$$

N, *M* and k_{max} are free parameters chosen by the analyst. The value *N* x *M* represents the number of matrix elements of ***X***. We chose the parameters *N*=100, *M*=100 and k_{max} = 8 on the basis of our preliminary analysis and experiences with the optimum choice of k_{max} value. Thus, each matrix was divided into smaller (*M* x *N*)-dimensional matrices (square windows).

FD values were calculated for each square window (window size *M* x *N* = 100 x 100 points), without overlap, using k_{max} = 8. Individual *FD* values from all square windows were averaged to obtain a final *FD* value for a particular image.

Fig. 1C, H show four square windows (each 100x100 points dimension) excised from sample images (Fig. 1B, G, respectively), while Fig. 1D and I represent numerical matrices corresponding to Fig. 1C and H, respectively, with surface representation (Fig. 1E ,J), respectively.

It is possible to calculate *FD* for whole images. However, this is not recommended if the image is an extremely inhomogeneous texture. In such case, the *FD* value does not represent the true measure, and division into square windows is advisable. All the calculations were performed with program routines in MatLab R2010a made by S. Spasić (2014.).

Statistical analysis: Two-way ANOVA was applied to test the differences between calculated *FD* values from 6 histological images in each of 2 time points during shoot organogenesis at 3 image resolutions (96, 192 and 384 pixel/inch). The dependent variable in the analysis was the *FD* value of the histological image. Therefore, we analyzed 36 images: 6 images per each developmental phase and resolution. Statistical analysis was performed with SPSS 13.0 for Windows.

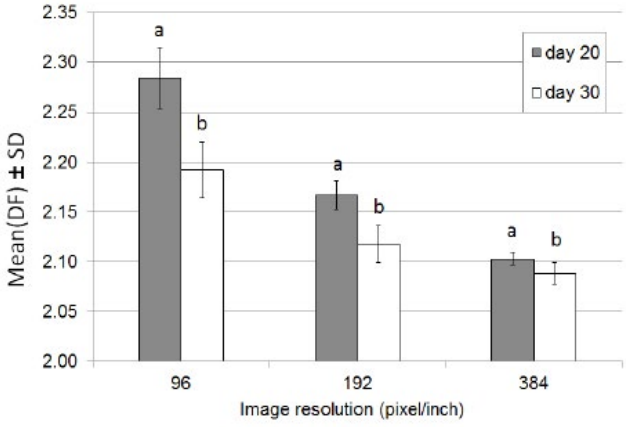

Figure 2. Mean (*FD*) ± SD values calculated from histological images (at different image resolutions: 96, 192 and 384 pixel/inch) obtained during *T. bellus* direct shoot organogenesis (n = 6). (a, b) - Different letters indicate significant differences between *FD* values in different subphases/days of organogenesis (α = 0.05).

RESULTS AND DISCUSSION

In Fig. 1, we present micrographs of *T. bellus* leaf explant sections showing meristemoids after the 20th (Fig. 1A, B) and 30th day (Fig. 1F, G) of direct shoot organogenesis. These meristemoids consisted of small isodiametric cells with prominent nucleus, while the cells underlying meristemoids were large and highly vacuolated. Frequent anticlinal and periclinal cell divisions within the meristemoids resulted in meristemoid elevation above the explant surface.

In microscopy, estimations of surface and volume in tissues differ when inspected at different resolutions (Paumgartner *et al*. 1981, Losa 2011). Therefore, the resolution of histological micrographs selected for fractal analysis was determined by the size of cell structures planned to be estimated. According to Rigaut (1984), boundaries of many irregular objects tend to behave like fractals at low resolution, but appear smooth (Euclidean) at very high resolutions, accounting precisely for the transition to the critical magnification. Increase in resolution is followed by a decrease in *FD* values, which was also evident in our results presented in Fig. 2.

We estimated *FD* values of "informative parts" of micrographs (Fig. 1B,C) at 3 resolutions each (96, 192 and 384 pixel/inch). Statistically significant decreases in *FD* values with progress of organogenesis was visible at all resolutions examined (Fig. 2). Therefore, fractal dimension quantitatively distinguished structures that characterized the early (20th) and late (30th day) meristemoid stages of shoot organogenesis at all three resolutions.

In a previous paper (Spasić 2014) it was shown that the method for 2D fractal analysis separated the main morphogenic stages of *T. bellus* direct shoot organogenesis. In the present work, we showed that this method is able to separate even more similar structures such as sub-stages of the selected morphogenic stage.

Although at all resolutions examined, fractal dimension values successfully discriminated between the observed meristemoids, we suggest a resolution of 96 pixel/inch as sufficient, due to the histological complexity of plant tissues.

Additionally, significant differences in *FD* values at two points of meristemoid devolopment indicate *T. bellus* direct shoot organogenesis to be a highly synchronized process.

CONCLUSION

The precision of our method for 2D fractal analysis was shown by quantitative separation of histological complexity characterizing early and late events of a single morphogenic stage of shoot organogenesis.

Our results indicate that a resolution of 96 pixel/inch was suitable for 2D fractal analysis of plant histological micrographs.

We suggest this method to be used for quantification of structure complexity in different growth and developmental processes in plants, as well as for the assessment of synchronization of selected processes. Our method is much simpler than other similar methods; it allows fast computational analysis of images and it can be used alone or in combination with other methods.

Acknowledgements — This work was supported by project OI 173045, 173017, 173015 financed by the Ministry of Education, Science and Technological Development of the Republic of Serbia.

REFERENCES

Alados CL, Escos J, Emlen TM & Freeman DC. 1999. Characterization of branch complexity by fractal analyses. Int. J. Plant Sci. **160**: 147-155.

Bruno MO, de Oliveira Plotze R, Falvo M & de Castro M. 2008. Fractal dimension applied to plant identification. Inform. Sci. **178**: 2722-2733.

Cross SS. 1997. Fractals in pathology. J. Patol. **182**: 1-8.

de Oliveira Plotze R, Falvo M, Pádua Juliano G, Bernacci LC, Maria V, Carneiro L & Oliveira G. 2005. Leaf shape analysis using the multiscale Minkowski fractal dimension, a new morphometric method: a study with Passiflora (Passifloraceae). Can. J. Bot. **83**: 287-301.

Jelinek FH & Fernandez E. 1998. Neurons and fractals: how reliable and useful are calculations of fractal dimensions. J. Neurosci. Meth. **81**: 9-18.

Landini G. 2011. Fractals in microscopy. J. Microsc. **241**: 1-8.

Losa GA. 2011. Fractals in biology and medicine. Encyclopedia of molecular cell biology and molecular medicine. Wiley-VCH Verlag GmbH & Co. KGaA.

Mandelbrot BB. 1982. The Fractal Geometry of Nature. Freeman, San Francisco.

Mandelbrot BB. 1975. On the geometry of homogeneous turbulence, with stress on the fractal dimension of isosurfaces of scalars. J. Fluid Mech. **72**: 401–416.

Mitrović A, Vinterhalter B & Ćulafić Lj. 2005. *In vitro* propagation of *Tacitus bellus.* J. Sci. Agric. Res. **66**: 33-39.

Mitrović A, Janosević D, Budimir S & Bogdanovic Pristov J. 2012. Changes in antioxidative enzymes activities during *Tacitus bellus* direct shoot organogenesis. Biol. Plant. **56**: 357-361.

Murashige T & Skoog F. 1962. A revised medium for rapid growth and bioassays with tobacco tissue cultures. Physiol. Plant. **15**: 473-497.

Paumgartner D, Losa G & Weibel ER. 1981. Resolution effect on the stereological estimation of surface and volume and its interpretation in terms of fractal dimensions. J. Microsc. **121**: 51–63.

Rigaut JP. 1984. An empirical formulation relating boundary lengths to resolution in specimens showing 'non-ideally fractal' dimensions. J. Microsc. **133**: 41–54.

Spasić S. 2014. On 2D Generalization of Higuchi's Fractal Dimension. Chaos, Solitons Fract. **69**: 179-187.

Sugimoto K, Gordon SP & Meyerowitz EM. 2011. Regeneration in plants and animals: dedifferentiation, transdifferentiation, or just differentiation. Trends Cell Biol. **21**: 212-218.

Xi EH & Zhao GJ. 2011. Research on differentiated xylem cells based on fractal dimension. BioResources **6**: 3066-3079.

Botanica SERBICA

REZIME

Ocena kompleksnosti meristemoida tokom *in vitro* organogeneze pupoljaka *Tacitus bellus* metodom 2D fraktalne analize

Sladjana Spasić, Aleksandra Mitrović, Dušica Janošević, Snežana Budimir

Ova studija se odnosi na analizu 2D fraktalnih karakteristika populacija ćelija koje učestvuju u formiranju meristemoida tokom *de novo* organogeneze pupoljaka u kulturi listova *Tacitus bellus*. U 2D fraktalnoj analizi korišćene su mikrografije koje predstavljaju ranu i kasnu fazu formiranja meristemoida. Analiza je pokazala da je složenost meristemoida u dve odabrane vremenske tačke razvića okarakterisana statistički značajno različitim vrednostima fraktalne dimenzije. Dobijeni rezultati pokazuju da je predloženi metod efikasan za fino razlikovanje histološki sličnih struktura pri odgovarajućoj rezoluciji mikrografije.

Ključne reči: 2D fraktalna dimenzija; organogeneza pupoljaka; *Tacitus bellus*